

Effect of Deposit Au Thin Layer Between Layers of Perovskite Solar Cell on Cell's Performance

Ahmed A. Assi^{1a*}, Wasan R. Saleh^{2b}, and Ezeddin Mohajerani^{3c}

^{1,2}Department of Physics, College of Science, University of Baghdad, Baghdad, Iraq

³Laser and Plasma Research Institute, Shahid Beheshti University, Tehran, Iran

^bE-mail: wasan_alazawi@yahoo.com, ^cE-mail: e-mohajerani@sbu.ac.ir

^{a*}Corresponding author: ahma.ali.asi@gmail.com

Abstract

The present work aims to fabricate n-i-p forward perovskite solar cell (PSC) with structure (FTO/compact TiO₂/compact TiO₂/ MAPbI₃ Perovskite/ hole transport layer/ Au). P3HT, CuI and Spiro-OMeTAD were used as hole transport layers. A nano film of 25 nm gold layer was deposited once between the perovskite (PSK) layer and the electron transport layer (ETL), then between hole transport layer (HTL) and the perovskite layer. The performance of the forward-perovskite solar cell was studied. The role of the electron transport layer and the hole transport layer in the perovskite solar cell was presented. The structural, morphological and electrical properties were studied with X-ray diffractometer (XRD), field emission scanning electron microscope (FE-SEM) and current-voltage (J-V) characteristic curves, respectively. J-V curves revealed that the deposition of the Au layer between the perovskite layer and electron transport layer reduced the power conversion efficiency from 3% to 0.08% when one layer of C. TiO₂ is deposited in the PSC and to 0.11% with two layers of C. TiO₂. Power conversion efficiency, with CuI as the hole transport layer, showed an increase from 0.5% to 2.7% when Au layer was deposited between PSK and CuI layers. Also, I_{sc} increased from 6.8 mA to 17.4 mA and V_{oc} from 0.3 V to 0.5V. With depositing Au layer between P3HT and PSK layers, the results showed an increase in the efficiency from 1% to 2.6% and an increase in I_{sc} from 10.7 mA to 30.5 mA, while V_{oc} decreased from 0.75 V to 0.5V.

Article Info.

Keywords:

perovskite solar cell, gold layer, CuI, P3HT, compact TiO₂

Article history:

Received: Aug. 10, 2021

Accepted: Oct. 04, 2021

Published: Dec. 01, 2021

1. Introduction

The last few years have seen an explosion of interest in photo-voltaic (PV) systems with an organic-inorganic lead halide perovskite active layer, that appeals to the technical community according to their high efficiency and inexpensive cost [1-3]. PV devices based on perovskite materials have demonstrated monotonic increase in power conversion efficiency (PCE) [4], rising from 3.9% when using CH₃NH₃PbBr₃ and CH₃NH₃PbI₃ as light absorbers in DSSCs with an iodine-based liquid electrolyte to over 20% [5, 6], with the current world record of 25.5 percent certified in 2021 by the National Renewable Energy Laboratory in the USA (NREL) [7].

The Perovskite Solar Cell (PSC) is consisted of five layers: hole transport layer (HTL), metal-based cathode, electron transport layer, perovskite as the absorber layer, and transparent conductive oxide (TCO) [8]. The transport layers are critical in determining a PSC performance. The hole transport layer (HTL) collects holes from the absorber layer and transports them to the cathode, where they are blocked by electrons.

To operate as a HTL, any substance must have a higher occupied molecular orbital (HOMO) than the perovskite absorber layer. Numerous hole transport layers (HTLs) have been employed, including PTAA, Spiro-OmeTAD, CuO, Cu₂O, Cui, and NiO [9]. While, the electron transport layer (ETL) collects electrons from the absorber layer and transports them to the anode, where they are blocked by holes. To be an ETL, a material's lowest unoccupied molecular orbital (LUMO) levels must be lower than those of the perovskite absorber layer. The ETL should have a high transparency in the UV-Visible range in order for all photons to passing through and then absorbed maximally by the absorber layer. Various ETLs are employed, including SiO₂, SnO₂, TiO₂, and ZnO [9].

The arrangement of the device is critical when assessing the overall performance of (PSCs). PSCs can further be classified into p-i-n (inverted) and n-i-p (regular or forward) structures based on the transport (electron/hole) material present on the outer portion of the cell/encountered by incident light [10]. For n-i-p structures, the conventional device structure of PSCs includes a transparent conducting electrode (Fluorine-doped tin oxide (FTO) or Indium tin oxide (ITO), an ETL, a perovskite (PSK) active layer, and a HTL. TiO₂, SnO₂, and ZnO are the most often utilized ETL materials, whereas Spiro-OMeTAD or the more stable Poly[bis(4-phenyl) (2,4,6-trimethylphenyl) amine is employed for the hole transport layer (PTAA) [11].

The fill factor (FF) usually used to quantify solar cell defects. It is defined as the ratio of the dark blue (maximum power output) to the light blue rectangles ($V_{oc}J_{sc}$), as appear in Fig. (1), and can be calculated as [12]:

$$FF = \frac{V_{MPP}J_{MPP}}{V_{oc}J_{sc}} = \frac{P_{MPP}}{V_{oc}J_{sc}} < 1 \quad (1)$$

where V_{MPP} is the voltage at maximum power output point, J_{MPP} is the current at maximum power output point, J_{sc} is the short-circuit current density, V_{oc} is the open-circuit voltage, and P_{MPP} is the maximum power output point.

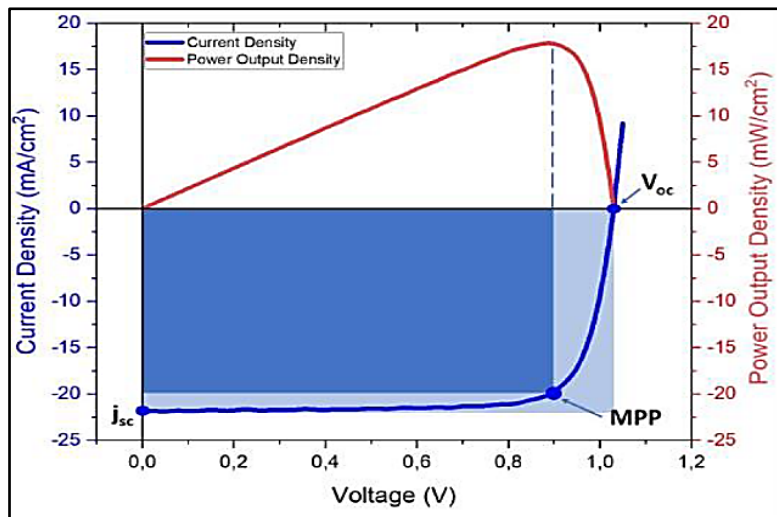


Figure 1: A solar cell's typical current density-voltage curve and matching electrical power output density. The current density (J) of the short-circuit, voltage (V_{oc}) of the open-circuit, and maximum power output point at (PMPP) are all denoted [13].

The most critical aspect of a solar system is its (PCE), which is defined as the ratio of the generated to the incident power and is computed using the following equation [12]:

$$PCE = \frac{P_{MPP}}{P_{incident}} = \frac{FF \cdot V_{oc} \cdot J_{sc}}{\Phi_E^{AM1.5G} \cdot A} \quad (2)$$

where $\Phi_E^{AM1.5G}$ is the power density of the sun on the Earth's surface, and A is the area of a solar cell.

This work is aimed to study the effect of gold nano-film on the performance of PCS when it is placed between perovskite layer and each of the electron and hole transport layers. Also, it demonstrates the importance of the hole transport layer and the electron transport layer in the cell when they are separated from the perovskite layer by a thin separator layer.

2. Experimental work

2.1. Chemical Materials

The used materials were fluorine doped tin oxide coated glass (FTO-glass), lead iodide (PbI₂), and methylamine iodide (MAI), which are from Sharifsolar Company. The titanium tetraisopropoxide (TTIP), ethanol, Hydrochloric acid (HCl), dimethyl sulfoxide (DMSO), dimethylformamide (DMF), chlorobenzene (CB), Lithium bis (trifluoromethanesulfonyl) imide (LITESI), acetonitrile, and Copper(I) iodide (CuI) are from Merck company. The Spiro- OMeTAD, Poly(3-hexylthiophene-2,5-diyl) (P3HT) are from Ossila company, and 4-tert-Butylpyridine, and 24 karat alloy gold (Au).

2.2. Preparation of solar cells layers

There are many steps to prepare perovskite solar cell layers. In this work, the method used was the same method used by A.A. Assi et al. [14, 15]. The conductive glass FTO/glass substrates were patterned by laser etching and sequentially washed with deionized water, detergent, acetone and isopropanol. Afterwards, the substrates were dried with nitrogen gas then left overnight in the oven at 60 °C to keep them dry and clean.

For the synthesis of C.TiO₂ layer two solutions were prepared: The first solution was prepared by adding 365µl titanium tetraisopropoxide (TTIP) to 2530 µl ethanol with stirring for one hr. at room temperature. The second solution was a mixture of 35µl of Hydrochloric acid (HCl) and 2530µl of ethanol. After 1 h, the second solution was slowly added to the first. The mixture was deposited on a clean FTO glass using spin coating in two steps: beginning first with a speed of 1500 rpm for 15 s and then with a speed of 4000 rpm for 25 s with acceleration 12 R-Time, then dried at a temperature of 140°C for 10 min. The thickness of each layer was approximately (200 - 250) nm. The second layer was added using spin coating (4000 rpm, the 30s, 12 R-Time) and then annealed at a temperature of 500°C for 30 min.

The perovskite layer was prepared by mixing 461 mg of lead iodide (PbI₂) with 159 mg of methylamine iodide (MAI) and dissolved in a solvent containing 78 mg of dimethyl sulfoxide (DMSO) and 600 mg of dimethylformamide (DMF). The mixture was stirred for 10 min at 100 °C then for extra 20 min. at room temperature. Spin coating was used for the deposition of the PSK layer in three steps: (2000 rpm) for 10s, (4000 rpm) for 10 s and the last step at 2000 rpm for 10s with dropwise adding of 200 µl of chlorobenzene (CB) as anti-solvent.

For hole transport layer, Spiro- OMeTAD was used, which was prepared using two solutions: The first solution, called S1, was prepared by mixing 72 mg of Spiro with 1 ml of CB and stirred for 1h with a stirrer. The second solution, called S2, consist of 520 mg of Lithium bis(trifluoromethanesulfonyl)imide (LITESI) mixed with 1 ml of acetonitrile and stirred for 1h with a stirrer. S1 was mixed with 17.5 ml of S2 and 28.8 µl of 4-tert-Butylpyridine and stirred for 20 min with a stirrer. The final mixture was filtered by 0.22 µm filter paper. The final solution was deposited using spin coating technique at 4000 rpm for the 20s.

Gold (Au) was deposited with a thickness between 70 - 100 nm as a cathode electrode using the thermal evaporation method. A hot plate at temperature 80 °C was used to remove the excess solvent.

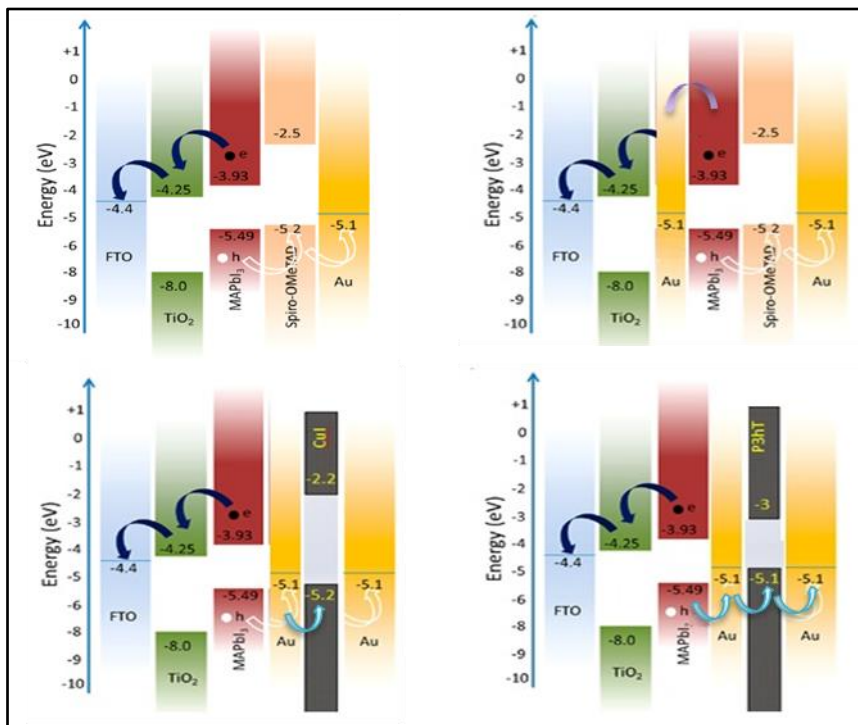


Figure 2: Energy diagram of a typical PSC using TiO_2 as the ETM, MAPbI_3 as the perovskite absorber, and Spiro-OMeTAD as the HTM. FTO is the front contact, while gold is the back contact [16].

Considering the energy levels shown in Fig. 2, it is obvious that the HOMO energy levels of P3HT, CuI, and spiro are 5.1 eV, 5.2 eV and 5.1 eV, respectively, which are very close. The HOMO for HTL should be higher than HOMO of perovskite layer. Also, it is noted that the Au work function is very close or similar to the HOMO of the prepared HTL. This result shows that the deposition of gold layer between perovskite layer and HTL can be used to improve the solar cells performance because of the work function of gold.

3. Results and discussion

The structure of the PSK layers were analyzed with a Shimadzu 6000 X-ray diffractometer, using $\text{Cu K}\alpha$ radiation of wavelength 1.5406\AA . The XRD patterns of the samples were recorded at a scanning rate of 0.08333° S-1 in the 2θ ranges (5° - 80°). Fig. 3 shows the XRD patterns of $\text{CH}_3\text{NH}_3\text{PbI}_3$ layer (PSK layers) with and without using chlorobenzene as anti-solvent.

The pattern has many peaks at 2θ equal to 14.2° , 20.17° , 23.66° , 24.69° , 28.63° , 31.01° , 32.04° , 35.16° , and 38.2° which corresponds to Miller indices (h k l) of (110), (112), (211), (202), (220), (213), (222), (042), and (213), respectively. The XRD measurements proved that the MAPbI_3 layer is of tetragonal structure. It can also be seen that chlorobenzene did not affect the structure of the perovskite layer.

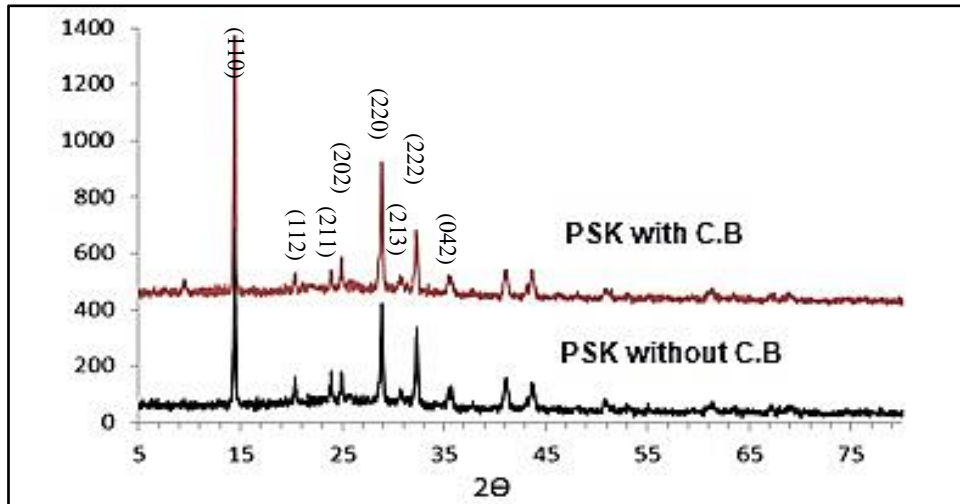


Figure 3: X-ray diffraction pattern of the PSK layer with and without using chlorobenzene as anti-solvent.

The XRD pattern of gold is shown in Fig. 4. The 2θ angles are 38.27° , 44.48° , 64.73° , 77.76° , 81.937° , 98.4° , 111.17° , 115.65° , corresponding to Miller indices (hkl) (111), (200), (202), (311), (222), (400), (313), (202), respectively. The XRD measurements denoted cubic structure space group Fm-3m, $a=4.069 \text{ \AA}$. The patterns and these results are in agreement with those of Oku [17].

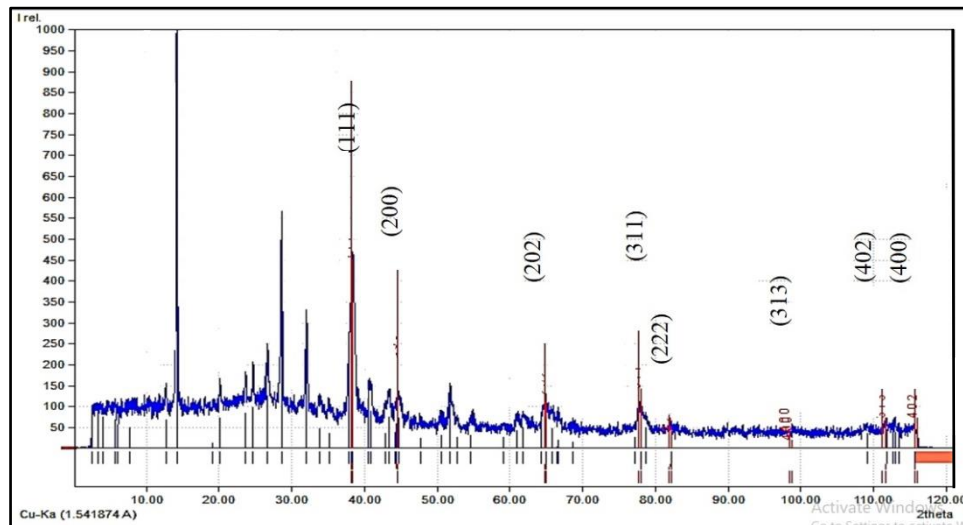


Figure 4: X-ray diffraction pattern of the PSK with gold electrode after one month.

The phase analysis for the X-ray diffractometer data was conducted using Match! Software for phase analysis data Version 3 from Crystal Impact-Software for Chemists and Material Scientists. The software compares the diffraction pattern of samples to a database which containing reference patterns to identify the phases which are present. In XRD Match! Software, there is not any available data for the structure containing Au interacted with the cell layers.

Figure 5 shows the FE-SEM images of perovskite layer prepared with chlorobenzene (Fig.5 a) and without chlorobenzene (Fig. 5 b) anti-solvent in 1 step method. Chlorobenzene was used in the process of preparing perovskite layer for improving the surface properties of the layer. From Fig. 5, it is revealed that using chlorobenzene resulted in a homogeneous layer with good topography.

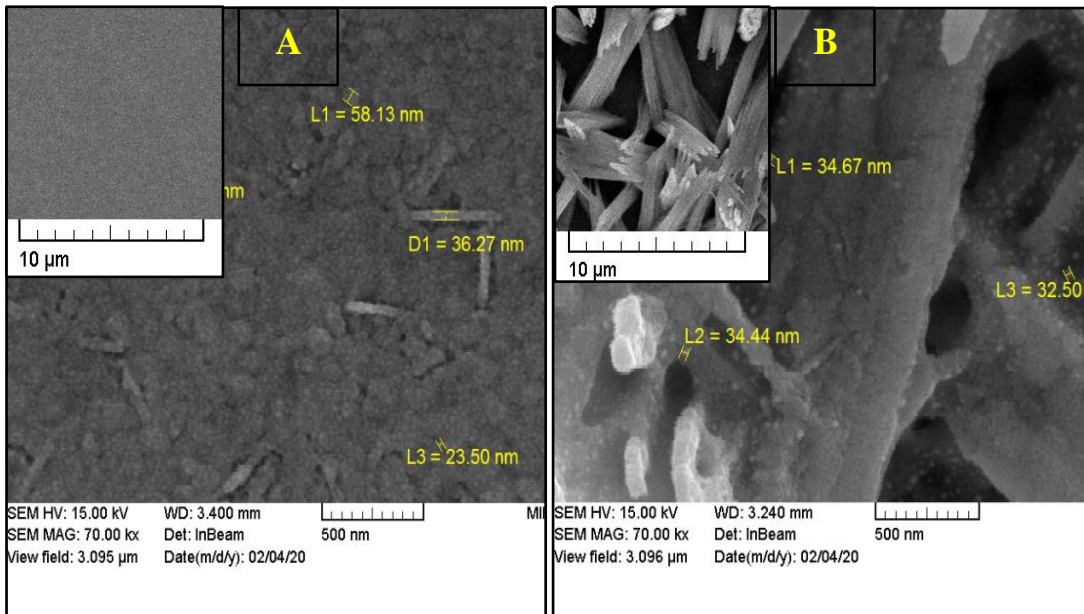


Figure 5: Top-view of FE-SEM images for PSK layer, A: PSK with C.B anti-solvent, B: PSK without C.B anti-solvent. L1, L2 and L3 are the grain sizes and D1 is the rod diameter.

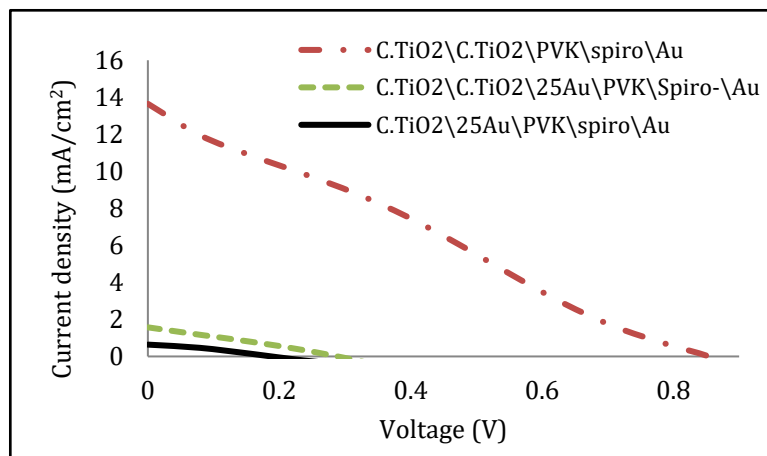


Figure 6: J-V characteristics of PSKs with thin Au layer between ETL and PSK.

Au layer of thickness 25 nm was deposited between ETL and PSK layer according to the structure in Table (1). The results of J-V characteristics of these structures (Fig. 6) show that the cells performance was reduced after depositing Au layer between ETL and PSK, which refer to the importance of ETL layer in the process of energy transformation in the solar cell.

The presence of the Au layer prevents the contact between ETL and PSK, but it does not cancel the ETL's role. The performance of PSC was also reduced when using one thin layer of ETL, which indicates that the ETL is essential in the functioning of the PSCs.

Table 1: Perovskite solar cell with thin Au layer between ETL and PSK Parameters.

ETL Type	V_{oc} (v)	J_{sc} (mA)	V_{max} (V)	I_{max} (mA)	F. F	η %
C.TiO ₂ \C.TiO ₂ \PSK\spiro\Au	0.55	13.65	0.40	7.55	0.40	3
C.TiO ₂ \C.TiO ₂ \25Au\PSK\spiro\Au	0.3	1.57	0.32	0.34	0.22	0.11
C.TiO ₂ \25Au\PSK\spiro\Au	0.24	0.64	0.32	0.14	0.29	0.08

A thin Au layer of thickness 25 nm was deposited between PSK layer and HTL. Two types of HTL were used: CuI and P3HT. Fig. 7 and Table (2) summarize the cell parameters measurements. It is clear that the efficiency of the cell with P3HT was lower than that with Spiro-OMeTAD. When Au layer was deposited between P3HT and PSK layer, the efficiency increased from 1 to 2.6, which is close to the efficiency with Spiro-OMeTAD. Also, I_{sc} was increased from 10.7 mA to 30.5 mA, but V_{oc} was decreased from 0.7 V to 0.5V.

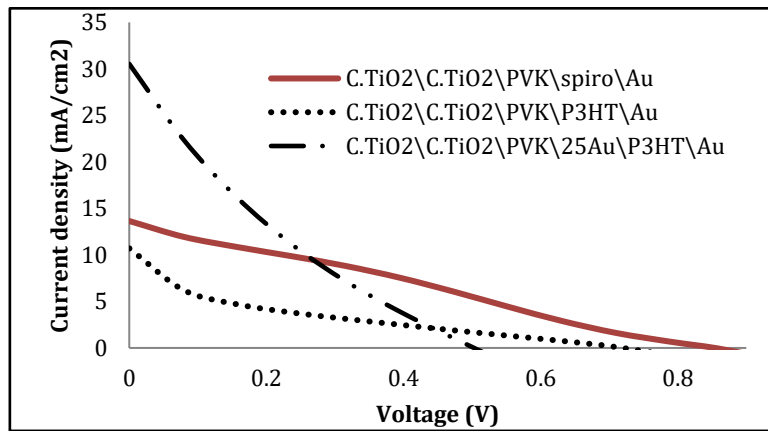


Figure 7: J-V characteristics of PSKs with thin Au layer between P3HT HTL and PSK.

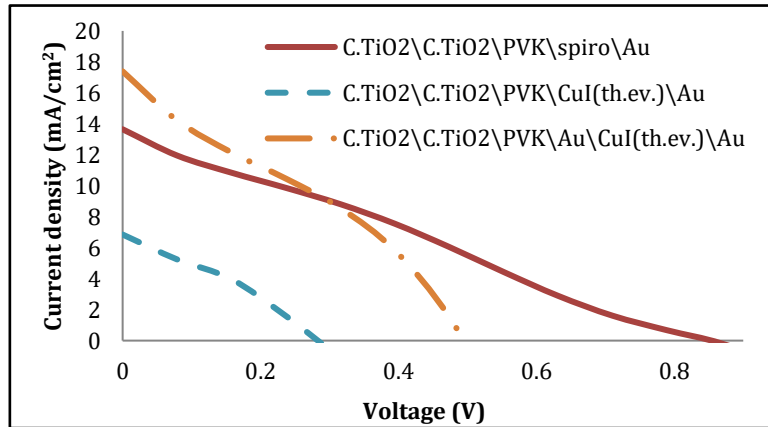


Figure 8: J-V characteristics of PSKs with thin Au layer between CuI as HTL and PSK.

Also, CuI was deposited, using thermal evaporation method, as the HTL and Au layer was deposited between CuI and PSK layers. The J-V characteristics of PSC with CuI HTL are shown in Fig. 8 and Table (2) where the efficiency has increased from 0.5% to 2.7% when 25 nm Au layer was deposited between PSK and CuI layer. It approaches the efficiency of PSC with Spiro-OMeTAD as the HTL. Furthermore, the I_{sc} increased from 6.8 mA to 17.4 mA and V_{oc} from 0.3 V to 0.5V.

Table 2: Perovskite solar cell parameters measured with thin Au layer between HTL and PSK.

ETL Type	V _{oc} (v)	J _{sc} (mA)	V _{max} (V)	I _{max} (mA)	F. F	η %
C.TiO ₂ \C.TiO ₂ \PSK\spiro\Au	0.55	13.65	0.40	7.55	0.40	3
C.TiO ₂ \C.TiO ₂ \PSK\CuI(th.ev.)\Au	0.30	6.85	0.32	1.59	0.23	0.50
C.TiO ₂ \C.TiO ₂ \PSK\Au\CuI(th.)\Au	0.50	17.39	0.32	8.55	0.28	2.70
C.TiO ₂ \C.TiO ₂ \PSK\P3HT\Au	0.75	10.71	0.32	3.13	0.12	0.99
C.TiO ₂ \C.TiO ₂ \PSK\25Au\P3HT\Au	0.50	30.54	0.24	11.14	0.16	2.64

From the results, one can conclude that depositing Au layer between the perovskite layer and ETL led to a significantly reduction in the efficiency of the solar cell. This refers that ETL has an essential role because Au layer prevents the direct contact between perovskite and ETL. This will increase the recombination and reduce visible light that is absorbed in the process of separating the electron-hole, which is formed in the PSK layer by the process of converting light energy.

On the other hand, using P3HT and CuI as HTL in PSC and depositing Au layer between the perovskite layer and the HTL has good effect on the cell efficiency, where the efficiency of the cell was improved by about 2.5 times (as concluded from the results of Fig. 7 and 8 and Table (2)). This indicates that the HTL may interact with the perovskite layer, but the gold layer prevented this interaction as well as improving the holes transfer process to the HTL.

4. Conclusions

A solar cell has been successfully fabricated with acceptable performance. To the best of our knowledge, this is the first time Au layer was added between the perovskite layer and the HTL and between the perovskite layer and the ETL. Inserting an Au layer between the perovskite layer and the HTL improved the efficiency of the cell by about 2.5 times more than the cell without Au layer. However, using P3HT and CuI as HTLs with an Au between ETL and perovskite layer reduced the efficiency. The ETL is essential in the function of the PSCs.

Acknowledgments

The authors would like to thank Photonics of the Physics department in the Colleges of Science, University of Baghdad for their valuable support and to provide the necessary facilities for research. Thanks, extended to the Organic Materials and Polymers (POMP) Laboratory in Shahid Beheshti University, Laser and Plasma Research Institute (LAPRI), for allowing us to use the preparation and examination devices available in Laboratory.

Conflict of interest

Authors declare that they have no conflict of interest.

References

1. Yu Z. and Sun L., *Recent progress on hole-transporting materials for emerging organometal halide perovskite solar cells*. *Advanced Energy Materials*, 2015. **5**(12): pp. 1500213.
2. Yusoff A.R.b.M. and Nazeeruddin M.K., *Organohalide lead perovskites for photovoltaic applications*. *The journal of physical chemistry letters*, 2016. **7**(5): pp. 851-866.

3. Chaudhary D.K., Kumar P., and Kumar L., *Realization of efficient perovskite solar cells with MEH: PPV hole transport layer*. Journal of Materials Science: Materials in Electronics, 2017. **28**(4): pp. 3451-3457.
4. Kodeary A., Hamidi S., and Moradlou R., *Voltage controlled properties of piezo-magneto-plasmonic core/shell nanoparticles*. Nano-Structures and Nano-Objects, 2020. **21**: pp. 100415.
5. Saliba M., Matsui T., Seo J.-Y., Domanski K., Correa-Baena J.-P., Nazeeruddin M.K., Zakeeruddin S.M., Tress W., Abate A., and Hagfeldt A., *Cesium-containing triple cation perovskite solar cells: improved stability, reproducibility and high efficiency*. Energy environmental science, 2016. **9**(6): pp. 1989-1997.
6. Wang Q., Phung N., Di Girolamo D., Vivo P., and Abate A., *Enhancement in lifespan of halide perovskite solar cells*. Energy Environmental Science, 2019. **12**(3): pp. 865-886.
7. Jeong J., Kim M., Seo J., Lu H., Ahlawat P., Mishra A., Yang Y., Hope M.A., Eickemeyer F.T., Kim M., et al., *Pseudo-halide anion engineering for α -FAPbI₃ perovskite solar cells*. Nature, 2021. **592**(7854): pp. 381-385.
8. Ng A., Ren Z., Shen Q., Cheung S.H., Gokkaya H.C., So S.K., Djurišić A.B., Wan Y., Wu X., and Surya C., *Crystal engineering for low defect density and high efficiency hybrid chemical vapor deposition grown perovskite solar cells*. ACS applied materials interfaces, 2016. **48**(8): pp. 32805-32814.
9. Roy P., Sinha N.K., Tiwari S., and Khare A., *A review on perovskite solar cells: Evolution of architecture, fabrication techniques, commercialization issues and status*. Solar Energy, 2020. **198**: pp. 665-688.
10. You J., Meng L., Song T.-B., Guo T.-F., Yang Y.M., Chang W.-H., Hong Z., Chen H., Zhou H., and Chen Q., *Improved air stability of perovskite solar cells via solution-processed metal oxide transport layers*. Nature nanotechnology, 2016. **11**(1): pp. 75-81.
11. Zhang P., Wu J., Zhang T., Wang Y., Liu D., Chen H., Ji L., Liu C., Ahmad W., and Chen Z.D., *Perovskite solar cells with ZnO electron-transporting materials*. Advanced Materials, 2018. **30**(3): pp. 1703737.
12. Faßl P., *Exploration of Properties, Stability and Reproducibility of Perovskite Solar Cells*, Ph. D. Thesis, RUPERTO-CAROLA UNIVERSITY OF HEIDELBERG, GERMANY, 2019.
13. Im J.-H., Lee C.-R., Lee J.-W., Park S.-W., and Park N.-G., *6.5% efficient perovskite quantum-dot-sensitized solar cell*. Nanoscale, 2011. **3**(10): pp. 4088-4093.
14. Assi A.A., Saleh W.R., and Mohajerani E., *Effect of Metals (Au, Ag, and Ni) as Cathode Electrode on Perovskite Solar Cells*. in *IOP Conference Series: Earth and Environmental Science*. 2021. IOP Publishing. No. 1, 012019, pp. 1-8.
15. Assi A.A., Saleh W.R., and Mohajerani E., *Investigate of TiO₂ and SnO₂ as electron transport layer for perovskite solar cells*. in *AIP Conference Proceedings*. 2020 .AIP Publishing LLC. No. 1, 050039, pp. 1-9.
16. Jena A.K., Kulkarni A., and Miyasaka T., *Halide perovskite photovoltaics: background, status, and future prospects*. Chemical reviews, 2019. **119**(5): pp. 3036-3103.
17. Oku T., *Crystal structures of CH₃NH₃PbI₃ and related perovskite compounds used for solar cells*. Solar Cells-New Approaches Reviews, 2015. **1**. ed.1, IntechOpen.

تأثير ترسيب طبقة رقيقة من الذهب بين طبقات خلية بيروفسكايت الشمسية على أداء الخلية

احمد علي عاصي¹ و وسن رشيد صالح² و عز الدين مهاجراني³

¹ قسم الفيزياء، كلية العلوم، جامعة بغداد، بغداد، العراق

³ معهد أبحاث الليزر والبلازما، جامعة شهيد بهشتي، طهران، إيران

الخلاصة

تهدف الدراسة الحالية إلى تصنيع خلية بيروفسكايت شمسية ذات تركيب امامي (forward n-i-p) بالتركيب (FTO/ compact TiO₂/ compact TiO₂/ MAPbI₃ Perovskite/ hole transport layer/ Au). تم استخدام P3HT و CuI و Spiro-OMeTAD كطبقات لنقل الفجوات (hole transport layers). تم ترسيب طبقة رقيقة 25 نانومتر من الذهب بين طبقة نقل الإلكترونات وطبقة البيروفسكايت ومن ثم ترسيب طبقة رقيقة من الذهب بين طبقة نقل الفجوات وطبقة البيروفسكايت. تمت دراسة أداء خلية البيروفسكايت الشمسية. كما تم عرض دور كل من طبقة نقل الإلكترونات وطبقة نقل الفجوات في خلية البيروفسكايت الشمسية. تمت دراسة الخواص التركيبية والمورفولوجية والكهربائية باستخدام مقياس حيود الأشعة السينية، والمجهر الإلكتروني الماسح للانبعاثات الميدانية ومنحنيات الجهد وكثافة التيار (J-V) على التوالي. كشفت منحنيات علاقة الجهد والتيار (J-V) أن ترسيب طبقة الذهب بين طبقة نقل الإلكترونات والبيروفسكايت قللت من كفاءة تحويل الطاقة من 3% إلى 0.08% عند ترسيب طبقة واحدة من ثنائي اوكسيد التيتانيوم المحكم و 0.11% عند ترسيب طبقتين من ثنائي اوكسيد التيتانيوم المحكم. بينما تظهر كفاءة تحويل الطاقة للخلية مع استخدام طبقة CuI كطبقة نقل الفجوات زيادة من 0.5% إلى 2.7% عند ترسيب طبقة الذهب بين طبقة البيروفسكايت وطبقة CuI وزيادة تيار الدائرة المغلقة (I_{sc}) من 6.8 مللي أمبير إلى 17.4 مللي أمبير وفولتية الدائرة المفتوحة (V_{oc}) من 0.3 فولت إلى 0.5 فولت. كما ان كفاءة تحويل الطاقة عند ترسيب طبقة الذهب بين طبقة P3HT وطبقة البيروفسكايت ازدادت من 1% إلى 2.6% حيث يزداد تيار الدائرة المغلقة (I_{sc}) من 10.7 مللي أمبير إلى 30.5 مللي أمبير لكن فولتية الدائرة المفتوحة تنخفض من 0.7 فولت إلى 0.5 فولت.